Naeiji, P., Woo, T. K., Ohmura, R., Alavi, S. (2022): Molecular dynamics simulations of interfacial structure, dynamics, and interfacial tension of tetrabutylammonium bromide aqueous solution in the presence of methane and carbon dioxide. - Journal of Chemical Physics, 157, 154702.

https://doi.org/10.1063/5.0106707

Molecular dynamics simulations of interfacial structure, dynamics, and interfacial tension of tetrabutylammonium bromide aqueous solution in the presence of methane and carbon dioxide

Parisa Naeji,[1,2] Tom K. Woo,[1] Ryo Ohmura,[3] Saman Alavi[1]

[1] Department of Chemistry and Biomolecular Sciences, University of Ottawa, Ottawa, Ontario K1A 0R6, Canada

[2] GFZ German Research Centre for Geosciences, Telegrafenberg, 14473 Potsdam, Germany

[3] Department of Mechanical Engineering, Keio University, 3-14-1 Hiyoshi, Kohoku-Ku, Yokohama 223-8522, Japan

Correspondence: rohmura@mech.keio,ac.jp, salavish@uottawa.ca

Abstract

The interfacial behavior of tetrabutylammonium bromide (TBAB) aqueous solutions in the absence of gas and presence of methane and carbon dioxide gases are studied by molecular dynamics simulations. The aqueous TBAB phase, at concentrations similar to the solid semiclathrate hydrate (1:38 mole ratio), has a smaller interfacial tension and an increase in the gas molecules adsorbed at the interface compared to the pure water. Both of these factors may contribute to facilitating the uptake of the gases into the solid phase during the process of semiclathrate hydrate formation. At similar gas pressures, CO_2 is adsorbed preferentially compared to CH_4, giving it a higher surface density due to the stronger intermolecular interactions of CO_2 molecules of the solution at the interface. The increase in relative adsorption of CH_4 at the solution surface compared to the pure water surface is due to the hydrophobic interactions between the n-alkyl chains of the TBA^+ cation and the methane gas.

Keywords: Interfacial tension; Gas adsorption; Tetrabutylammonium bromide aqueous solutions; Methane; Carbon dioxide; Gas hydrate; Semiclathrate hydrate.

I. INTRODUCTION

The ionic clathrate hydrates or semiclathrates, such as those of quaternary ammonium and phosphonium salts, have been intensively studied over the past few years, with particular attention being paid to tetrabutylammonium bromide (TBAB), tetra-*n*-butylammonium chloride (TBAC), tetra-*n*-butylphosphonium bromide (TBPB), and tetra-*n*-butylphosphonium chloride (TBPC) due to their lower toxicity and stability under mild pressure and temperature conditions.[1-3]

Tetrabutylammonium bromide semiclathrates are a class of crystalline inclusion compounds in which the cage framework consists of water molecules and bromide anions, while the TBA^+ cations occupy large T_2P_2 cages in the framework made from merging of two tetrakaidecahedral (T) and two pentakaidecahedral (P) cages of the canonical clathrate hydrate structures.[3] The stoichiometry of the orthorhombic semiclathrate hydrate unit cell is $2TBAB{\cdot}76H_2O$. The framework also has six dodecahedral (D) cages per unit cell which can be filled if small gas molecules are present at sufficient pressure at the time of semiclathrate hydrate formation. This aspect is similar to canonical clathrate hydrates where the cages are formed solely by water molecules.[4] An incentive to study TBAB semiclathrate hydrate as a prospective energy storage medium is the property of this substance to include such small gases as methane, carbon dioxide, and hydrogen in the empty D cages at pressures lower than the canonical clathrate hydrates of these gases.[5,6] In particular, the TBAB semiclathrate hydrate encages methane under milder conditions compared to methane-containing canonical gas hydrates and therefore effectively improves the stability conditions of methane gas storage. Among the semiclathrate hydrates, particular attention has been paid to TBAB as a prospective thermodynamic hydrate promoter within the past decade.[7,8]

Since the semiclathrate hydrate first forms at the interface of TBAB aqueous solution / guest gas phase, the interfacial behaviors such as surface tension become important in determining details of the solid semihydrate phase formation. The surface tension of water is usually affected by adding additives such as electrolytes (increasing effect) and surfactants (decreasing effect).[9-11] The tetrabutylammonium halides are classified as electrolytes and the surface tension of their aqueous phases, especially TBAB solutions, in the presence of gas phases were studied by some researchers.[12-15] The surface activity of TBAX solutions is markedly dependent on the nature of their counterions, just as with other electrolytes in aqueous solutions.[14] Nashed et al. concluded that tetrabutylammonium hydroxide (TBAOH) can reduce the gas/liquid surface tension and enlarge the gas/liquid contact area. This causes a decrease in the mass transfer resistance between hydrate formers and water and thus an increase in the gas solubility and diffusivity in the aqueous phase. Therefore, TBAOH can have dual functionality as a thermodynamic promoter and as a kinetic promoter for gas uptake.[8] On the other hand, TBAOH has been found efficient for the inhibition of CH_4 and CO_2 hydrates. The shorter alkyl chains in the cationic part of ionic liquids offer superior thermodynamic inhibition. The aqueous TBAOH solutions were able to perform well for the studied systems due to their surface-active nature, so that allows them to adhere at the gas/liquid interface. [10]

The measurement of surface tension of TBAB aqueous solution under gas pressure was specifically carried out by Massoudi and King about forty years ago. They reported the decrease in surface tension of the TBAB solution at 25 ℃ when in contact with the gases CH_4, C_2H_4, C_3H_8, n-C_4H_{10}, CO_2 and N_2O. The decrease in surface tension was observed to be a sensitive function of the TBAB electrolyte concentration.[15]

In the case of tetrabutylammonium halide aqueous solutions, it is important to know the effect of surface adsorption from both the liquid and gas phases of the interface on the surface thermodynamics. In the liquid phase, the surface adsorption is a hydrophobic effect; that is, by the transfer of the large hydrophobic TBA^+ ions from inside the aqueous solution phase to the surface, the ordered water clusters (icebergs) solvating the nonpolar groups of the electrolyte are freed to return to the bulk solution.[14] Massoudi and King found that the presence of TBAB exerts a significant effect on the adsorption of the gases at the aqueous interface. Hydrophobic interactions were observed between adsorbed gas molecules and TBA^+ cations concentrated at the interface. As a result, the change in surface tension with pressure of hydrocarbon gases was found to be larger for TBAB solutions than for pure water, however, the opposite was found in the case of CO_2.[15] The surface tension between gas (CO_2 and N_2) and TBAB aqueous solution was specifically measured by Akiba and Ohmura.[12,13] They found that the values of the surface tension of the CO_2-TBAB(aq) solutions were smaller than the air-TBAB(aq) solutions and CO_2-water system with similar gas pressure and TBAB concentration. The surface tension decreased with increasing CO_2 pressure and mass fraction of TBAB in the aqueous solution indicating that more TBA^+ ions are adsorbed at the interface. [12] The depletion of surface tension with increasing mass fraction of TBAB in the CO_2+N_2+TBAB(aq) system is consistent with that in the CO_2+TBAB(aq) system. However, the pressure gradient of the surface tension mainly depends on the chemical species of the gas phase.[13] Sarlak et al. also reported the similar results for CO_2+TBAB(aq) system with or without the presence of surfactant. [16]

Molecular dynamics (MD) simulations contribute to understanding the microscopic mechanism of action of tetrabutylammonium aqueous solutions at the gas/water surface and its effect on the surface tension. There are a few MD simulation studies of solid TBAB or other

tetrabutylammonium halide semiclathrate hydrates in the presence of gas molecules.[6, 17,18] These studies did not specifically study the interface behaviors in these systems. Muromachi et al. showed that the physical adsorption properties of clathrate hydrates for developing gas capture technology can be further improved by crystal engineering with ionic guests.[6] Nguyen et al. confirmed that the water perturbation by TBA^+ in the bulk is attributed to the promotion effect of high TBAB concentration on CO_2 hydrate formation.[19] In this work, we study the interfacial properties, including surface tension, of TBAB aqueous solutions in the presence of pure methane and carbon dioxide and their mixtures under different gas phase thermodynamic conditions. The predicted trends in the interfacial tensions are compared with experimental values and the microscopic structure of the solutions and interface are used to describe these trends. Implications on the semiclathrate hydrate phase formation are discussed.

II. SIMULATION METHODS

Molecular dynamics simulations were performed using the DL_POLY program version 2.20 developed by Smith, Forester, and Todorov.[20] The TBAB solutions were simulated at 273.15 and 298.15 K, and a range of pressures based on the number of CH_4 and CO_2 molecules in the gas phase for the constant volume simulations.

The intermolecular interactions of water molecules were modeled with the TIP4P/2005 potential,[21] CH_4 was represented by the TraPPE united atom potential[22] and CO_2 with TraPPE rigid model.[23] The GAFF (General AMBER Force Field)[24] was employed for TBAB molecules to determine the Lennard-Jones parameters for van der Waals interactions and the nucleus-centered point charges for the electrostatic interactions were determined by using the CHELPG method.[25] The potential parameters used in the simulations are given in Table I. The standard

Lorentz-Berthelot combining rules were adopted for unlike pairs of atoms in particular, $\varepsilon_{ij} = (\varepsilon_{ij} \times \varepsilon_{jj})^{1/2}$ and $\sigma_{ij} = (\sigma_{ij} + \sigma_{jj})/2$.[26] A long cutoff radius of 23 Å was chosen for the van der Waals interactions to give converged values of the interfacial tension for pure water and water/CH_4 and water/CO_2 systems. Our previous work showed that with this cutoff, long-range corrections to the interfacial tension are small.[27,28] Long-range electrostatic interactions were handled using the Ewald method with a relative error of 10^{-6}.

TABLE I. Force field parameters used in the simulations.[21-24]

Molecule	**Atom**	***σ* / Å**	***ε* / kcal.mol^{-1}**	***q* / *e***
H_2O	O	3.159	0.1852	0.0000
	H	0.0000	0.0000	0.5564
	M	0.0000	0.0000	-1.1128
CO_2	C	2.800	0.0536	0.7000
	O	3.050	0.1569	-0.3500
CH_4(UA)	C	3.730	0.2941	0.0000
TBA^+	C	3.340	0.1090	-1.3360[a]
	H	H(CH_3): 1.960	0.0160	1.7760[a]
		H(CH_2): 2.649		
	N	3.250	0.1700	0.5600
Br^-		3.97	0.2055	-1.0000

[a] Sum of charges of all C or H atoms.

The combinations of force fields for water, methane, carbon dioxide, and TBAB have been previously used in simulations of CH_4 clathrate hydrate, CO_2 clathrate hydrate, and TBAB

semiclathrate hydrate phases and have been shown to give good agreement with phase diagrams and other thermodynamic and mechanical properties of the phases.[6, 18, 29, 30]

To prepare a TBAB aqueous solution with the same composition as the orthorhombic semi-hydrate phase, a 4×4×2 unit cell replica of TBAB semiclathrate hydrate, containing 2432 water molecules and 64 TBAB molecules, was placed in the center of a simulation box of dimension around 48×50×100 $Å^3$ and completely melted at 500 K using the *NVT* ensemble with a thermostat relaxation time of 0.2 ps. Periodic boundary conditions were applied in all directions. This system was cooled to 298 K for 2 ns, and finally was equilibrated for 2 ns to a temperature of 273 K where the semiclathrate is formed from the aqueous solution. The initial solid starting structure and melted solutions are shown in Figure S1 of the Supplementary Material.

To determine surface properties of free water-TBAB solutions with the same composition as the semiclathrate hydrate phase, an interface was generated by adding empty space in the *z*-direction to the solutions prepared previously and the system was allowed to equilibrate over 2 ns. The configuration of simulation set-up for the TBAB solution with exposed surfaces after equilibration is shown in Fig. 1(a). Compared to Fig.S1 of the Supplementary Material, the distribution of the TBA^+ and Br^- ions in the solution are no longer isotropic and the TBA^+ ions preferentially aggregate at the solution interface. Simulations of the solution exposed to vacuum were conducted to determine the interfacial tension of the solutions and to validate the computational methodology at each temperature. Viewed perpendicular to the free surface (perpendicular to the *xy*-plane), the right-hand panel of Fig. 1(a) shows that the outer solution surface has both water and TBA^+ ions exposed.

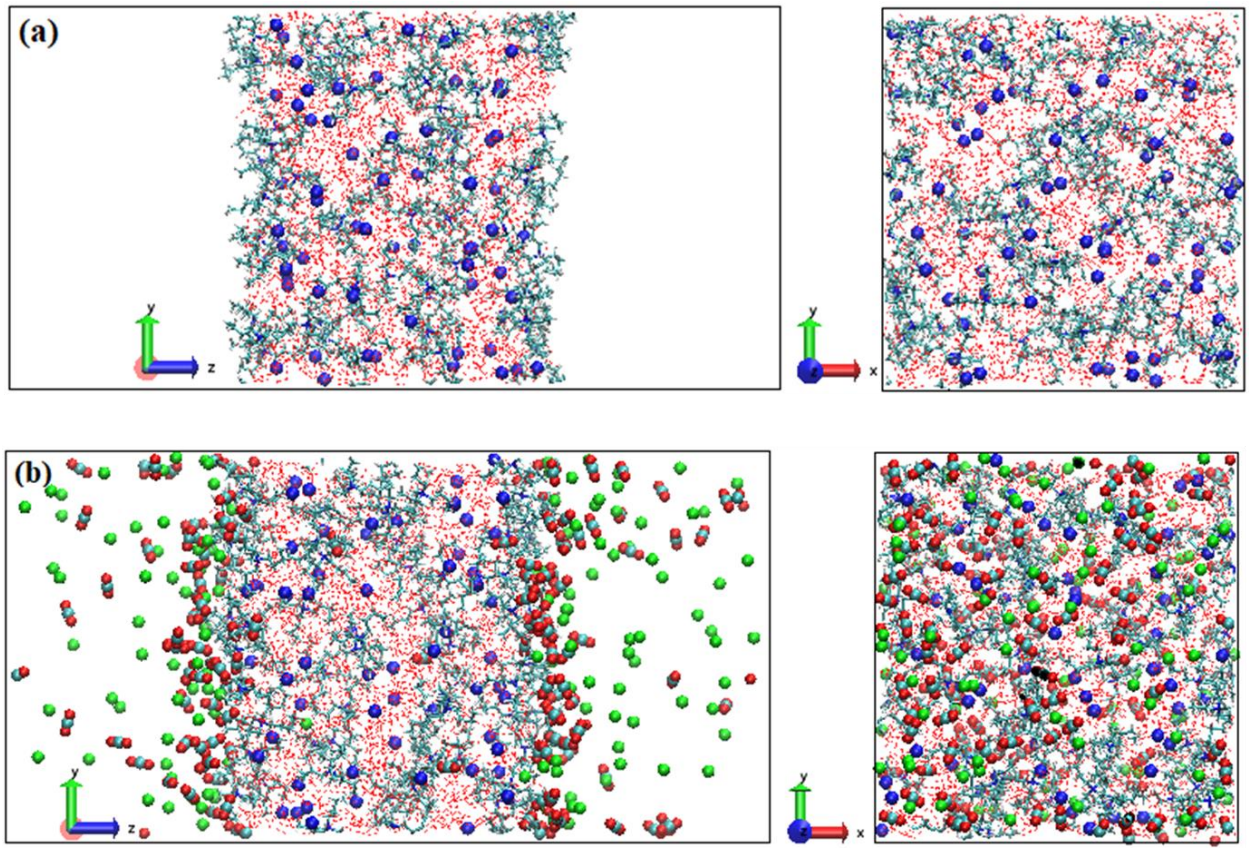

FIG. 1. (a) The initial configuration of the equilibrated TBAB aqueous solution at 273 K with exposed surfaces along the *xy*-plane viewed in the *yz*- and *xy*-planes. Water molecules are represented by their hydrogen bonding with red dashed lines. TBA^+ ions are shown with blue line structures and Br^- ions are represented by violet spheres. (b) The TBAB solution is placed in the center of the simulation cell and the CH_4 (green atoms) and CO_2 (cyan and red atoms) molecules are equilibrated on both sides of the water phase along the *z*-direction.

Gas molecules were added randomly into the empty space in the *z*-direction around the aqueous solution phase in the simulation cell and allowed to relax at a temperature 400 K using *NVE* ensemble simulations while the TBAB and water molecules were frozen. The gas and

solution were equilibrated for 100 ps using *NVT* ensemble at the desired temperature and pressure before the data collection from the simulation began. The equilibrated system was then simulated up to 2 ns to gather data for the calculations of the gas-solution interfacial properties. The convergence of the simulations was verified by plotting the time dependence of the total potential energy (E_{conf}) and the pressure of the system in Fig. S2 of the Supplementary Material. A snapshot of the final configuration of the simulation of the TBAB solution with CH_4 and CO_2 gas mixture is shown in Fig. 1(b).

The hydrostatic pressure for the simulation systems with gas molecules is controlled by inserting different numbers of gas molecules in the empty space of the simulation. The hydrostatic pressure is determined from the mean value of the P_{zz} component of the pressure tensor. The uncertainty in the hydrostatic pressure is estimated as the standard deviation of this mean tensor component.

The *z*-density profiles for water, TBA^+, Br^- and the gas species were calculated from the equilibrated simulations and the location of the interface was determined from the position of the Gibbs dividing surface for water molecules. The boundary of the gas phase was specified by the locations where the *z*-density of water effectively becomes zero on both sides of the liquid phase. The average number of gas molecules within the gas phase volume at each temperature was determined.

The interfacial tension, γ, for the solution/vacuum and solution/gas systems is determined by the use of the pressure tensor,

$$\gamma = \frac{L_z}{2}\left(P_{zz} - \frac{P_{xx} + P_{yy}}{2}\right), \quad (1)$$

where (P_{xx}, P_{yy}) and P_{zz} are the mean values of the tangential and normal components of the pressure tensor of the simulation cell along the *x*-, *y*- and *z*-directions, respectively, and L_z is the length of the simulated box along the *z*-direction normal to the interface. [31-37]

III. RESULTS AND DISCUSSION

Figure 2 shows the *z*-density profiles for water, Br^-, and TBA^+ (for the N and C atoms) in the aqueous solution in the absence of gases at the interface at 273.15 K. The *z*-density profile of a pure water phase at the same temperature is given for comparison. The *z*-density in the pure water phase is uniform inside the bulk and drops sharply at the interface. In contrast, the *z*-density for water is non-uniform throughout the slab in the TBAB solution, with higher density near the solution-vacuum interface. The TBA^+ and Br^- ions are inhomogeneously distributed in the solution with respect to the *z*-direction normal to the interface, with the TBA^+ ions in greatest density at the interface and the Br^- ions associated with the density peaks of the water molecules. This behavior is seen qualitatively in Fig. 1 where micro-domains of the salt and water are observed. The peaks in the *z*-density for TBA^+ and Br^- alternate in the *z*–direction which optimizes the electrostatic interactions in the solution. Both ions have a higher *z*-density at the interface than in the bulk of the solution.

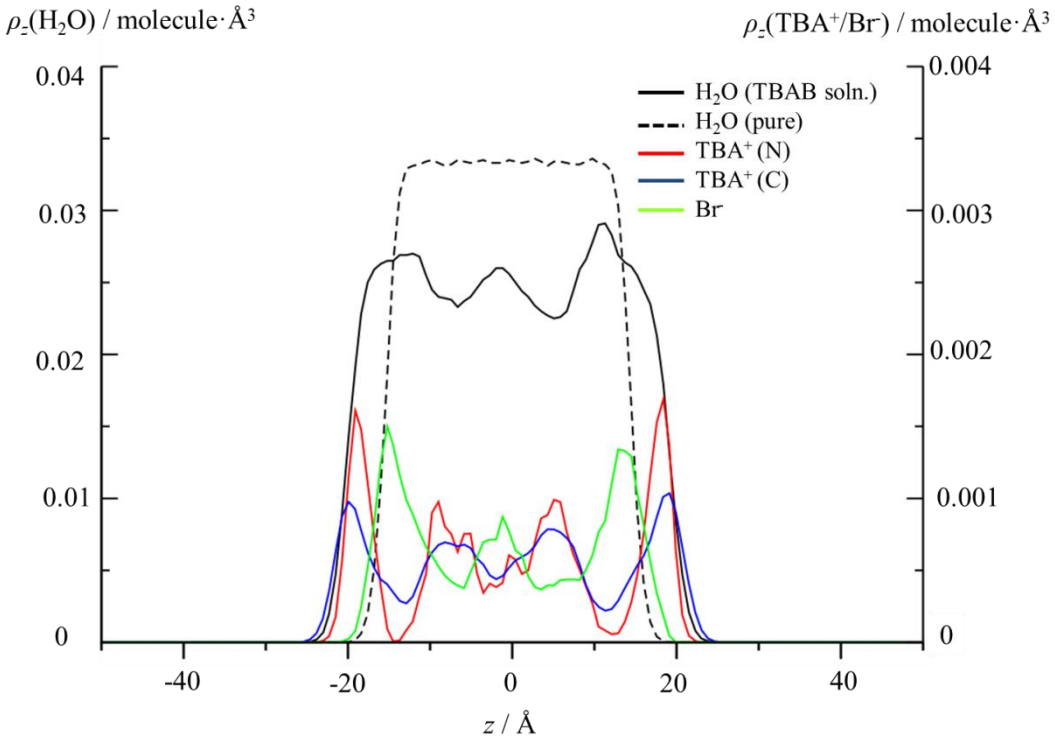

FIG. 2. The *z*-density profiles for water, Br^-, and TBA^+ (N at C atoms) in the TBAB(aq) solution at 273.15 K. The *z*-density profile of the pure water surface at the same temperature is given for comparison.

Traces from snapshots of the motion of Br^- and TBA^+ ions in the TBAB(aq) solution separated by consecutive 0.5 ps intervals over a total time of 0.5 ns after equilibration are shown in Fig. 3(a), and (b), respectively. Within this time frame, the ions remain within the same domain of the solution which is consistent with the inhomogeneous spatial distribution shown in their *z*-density profiles in Fig. 2. Tamaki (1967) suggested that structurally ordered "icebergs" of water molecules form around the nonpolar groups (alkyl groups) of the cations in bulk solution. Upon formation of an interface, the hydrophobic TBA^+ ions are transported to the surface of the system and the solvating water molecules are released back into the liquid aqueous solution. The

TBA^+ ions show a tendency to be rejected from the aqueous phase as a result of this strong cohesive force of water-water bonding.[14] As seen in Fig. 3, it is clear that there are a larger number of TBA^+ ions at the interface compared to hydrophilic Br^- ions.

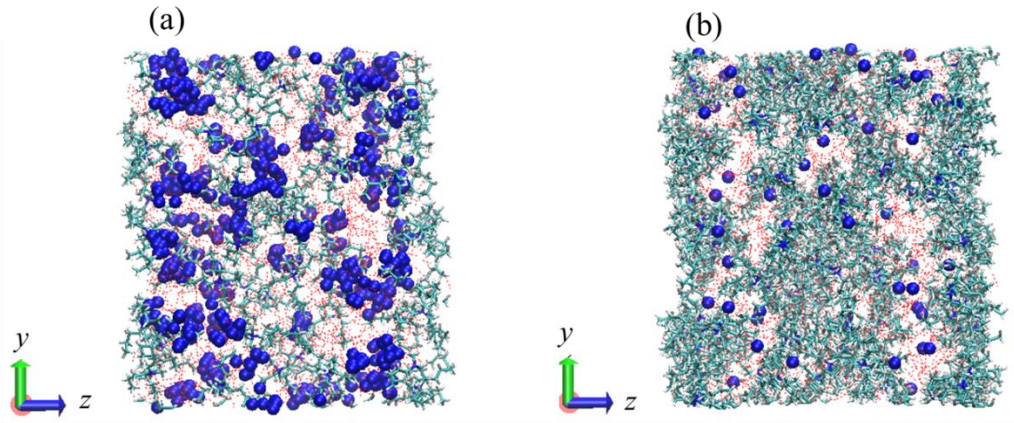

FIG. 3. Snapshots over 0.5 ns of the motion of (a) Br^- and (b) TBA^+ ions in the TBAB(aq) solution system at 298.15 K. The *xy*-plane forms the interface of the solution. In these figures, other molecules are shown fixed in their initial positions. Within the simulation time, the ions remain in specific domains, consistent with the *z*-density plot of Fig. 2.

The interfacial tensions calculated for the TBAB(aq) solutions are given in Table II. At each temperature, the TBAB(aq) interfacial tension is less than that of pure water, 67.6 compared to 70.1 $mN \cdot m^{-1}$ at 273.15 K, and 57.5 compared to 68.4 $mN \cdot m^{-1}$ at 298.15 K, respectively. The presence of TBAB in the solution leads to a decrease of 7-30% in the surface tension. These trends are consistent with experimental data, where higher concentrations of TBA-based salts lead to a decrease in the surface tension of the solution, due to the weaker intermolecular interactions between the hydrophobic ionic components and water molecules at the interface compared with the pure water interface.[38] This is in contrast to aqueous solutions of simple inorganic salts such as NaCl which have larger interfacial tensions than the pure water phase.[39]

TABLE II. The calculated interfacial tension, γ, ($mN \cdot m^{-1}$) along with uncertainties at 273.15 and 298.15 K for the TBAB(aq) solution exposed to vacuum and at different hydrostatic pressures, P_{zz} (bar), of CH_4 and CO_2 (with uncertainties of 0.1 bar). The total number of gas molecules in the simulation, N_{gas}(tot), required to generate the stated gas pressure is given for each simulation along with the average number of adsorbed gas molecules at the TBAB(aq)/gas interface, $\langle N_{gas}(ad) \rangle$. Interfacial tensions of H_2O/gas interfaces at similar pressures are given for comparison.

System	273.15 K				298.15 K			
	P_{zz}	N_{gas}(tot)	$\langle N_{gas}(ad) \rangle$	γ	P_{zz}	N_{gas}(tot)	$\langle N_{gas}(ad) \rangle$	Γ
TBAB(aq)	0.0	0	0	68±1	0.0	0	0	58±1
H_2O	0.0	0	0	70±1	0.0	0	0	68±1
TBAB(aq)/CH_4	1.7	133	63	65±1	5.4	133	53	55±1
	22.6	266	115	62±1	30.4	266	101	48±1
H_2O/CH_4	17.9	133	47	68±1	6.2	45	14	65±1
					34.8	106	19	62±1*
TBAB(aq) /CO_2	1.5	350	267	51±1	4.9	266	176	44±1
	3.7	400	300	44±1	15.2	400	257	42±1
	4.7	450	338	42±1				
H_2O/CO_2	5.6	133	101	64±1	5.0	50	27	61±1*

* From Ref. [28]

Figure 4 shows the *z*-density profiles for water, CH_4, CO_2, Br^-, and TBA^+ (C atoms) in the TBAB(aq)/CH_4 and TBAB(aq)/CO_2 system at 298.15 K and approximately 5 bar. Figure S3 and Fig. S4 show the results for TBA^+ (atom N) and system at higher pressures, respectively. Water molecules have similar *z*-density plots in TBAB(aq)/CH_4 in Fig. 4(a) and TBAB(aq)/CO_2 in Fig. 4(c). The *z*-density of the TBA^+ cations increases slightly at the interface (with sharper edges) in the presence of the non-polar CH_4 gas compared with that of the solution exposed to CO_2. Figures 4(b) and 4(d) (and also Fig. S4(b)) show that at comparable gas pressures, the *z*-density of CH_4 and CO_2 gas molecules at the interface are greater in the TBAB(aq) solutions than for the pure water phase. The absolute increase in surface density compared to the water phase for CO_2 is greater than CH_4 at the TBAB(aq) interface, but the proportional increase of surface adsorption of CH_4 is larger at the TBAB(aq) interface.[23] The *z*-density of both gas molecules increases at the solution interface as the gas pressure increases. The increased gas adsorption at the TBAB(aq) interface compared to the pure water interface is related to the stronger interaction energies of the gas molecules with hydrophobic TBA^+ groups which are present at high concentrations at the interface.

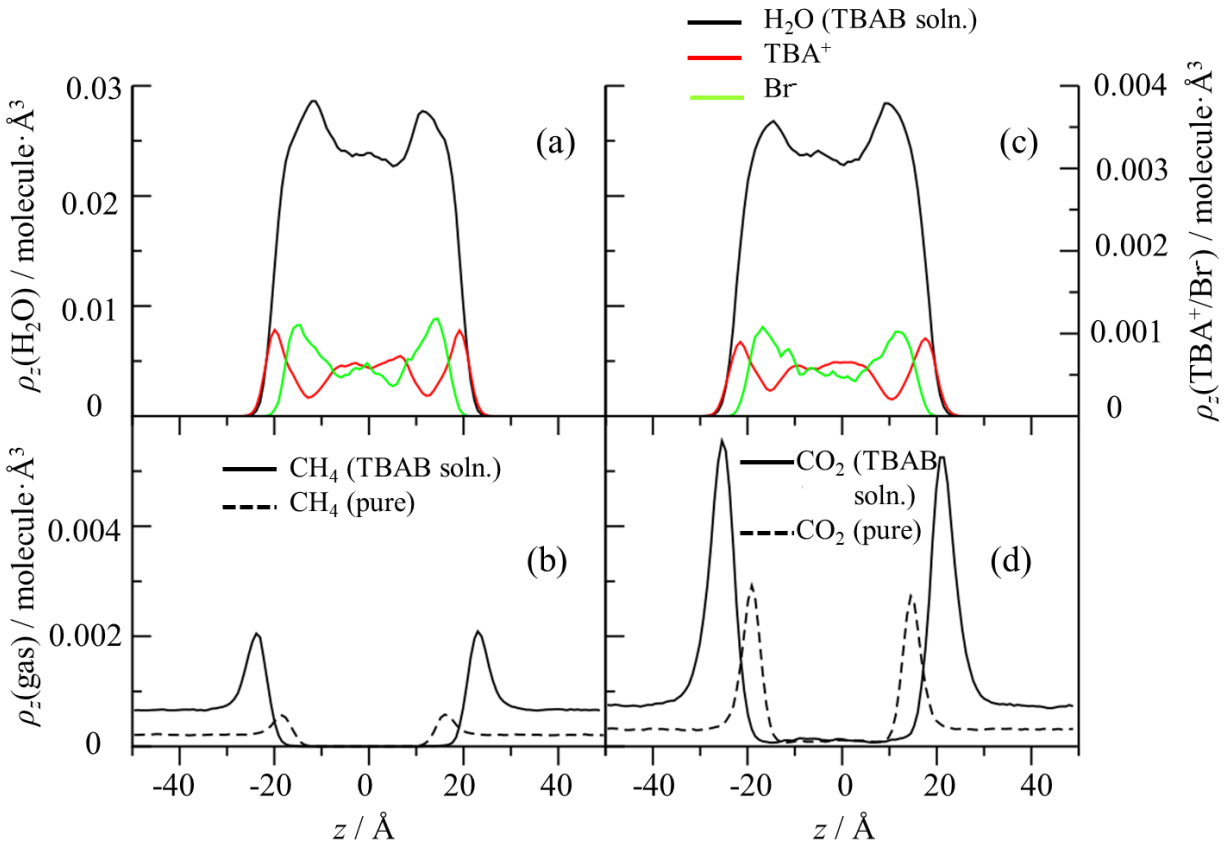

FIG. 4. The *z*-density profiles in the TBAB(aq)/CH_4 system for (a) water, Br^-, and TBA^+ (atom C) and (b) CH_4 at 5.4 bar. The *z*-density profiles in the TBAB(aq)/CO_2 system for (c) water, Br^-, and TBA^+ (atom C) and (d) CO_2 at 4.9 bar under 298.15 K. The *z*-density profiles for the CH_4 and CO_2 at the interface of a pure water system at similar pressures are also given in (b) and (d).

The snapshots of the TBAB(aq) systems in contact with CH_4 and CO_2 gas after equilibration given in Figs. 5(a)-5(b), clearly show the excess gas density at the interface compared to the bulk gas phase. Zoomed views of the interfaces, which show the interactions of the gases with the n-butyl groups of TBA^+ are shown in Fig. S5 of the Supplementary Material. Note the dissolution of some gas phase molecules (in particular CO_2) in the solution phases in each case. In the range of gas pressures used, full monolayer coverage of gas at the interface is

not observed. As seen in traces of selected gas molecules shown in Figs. 5(c) and 5(d), surface adsorbed molecules are in dynamic equilibrium with those in the gas phase. The exchange of molecules between the gas and interface occurs repeatedly in the nanosecond timescale of the simulation. This behavior is similar to our previous observations of methane and carbon dioxide on pure water surfaces.[22,23]

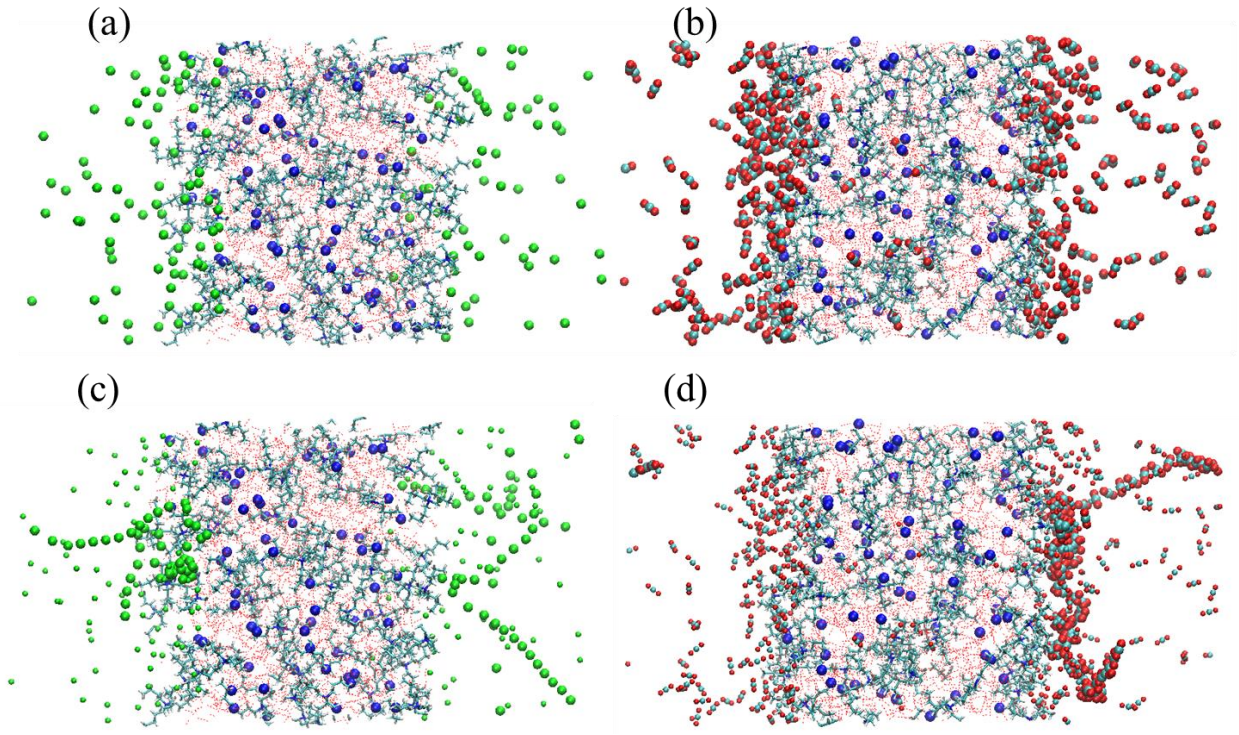

FIG. 5. Snapshots of the equilibrated TBAB(aq)/gas simulations for (a) CH_4 and (b) CO_2, which show aggregation of the gas molecules at the solution interfaces. Traces of the motion of individual (c) CH_4 and (d) CO_2 molecules at the TBAB(aq) interfaces over 0.5 ns at 298.15 K and pressure of ~5 bar. The absorption and release of the gases from the interface are observed.

Figure 6 shows the variation of the interfacial tension as a function of hydrostatic pressures up to 30 bar for the TBAB(aq)/gas systems at two temperatures. The interfacial

tensions are higher at lower temperature, as expected. At similar gas pressures, the interfacial tensions of TBAB(aq)/CO_2 are considerably lower than TBAB(aq)/CH_4. In the temperature and pressure range of Fig. 6, the CO_2 gas does not condense to liquid and the significant decrease in interfacial tension for TBAB(aq) is related to CO_2 surface adsorption. Although both gases show wetting behavior on the interface, as seen in Table II more CO_2 molecules are adsorbed at the gas-solution interfaces than CH_4, a result similar to our previous work for gas-pure water systems.[23]

systems.[28]

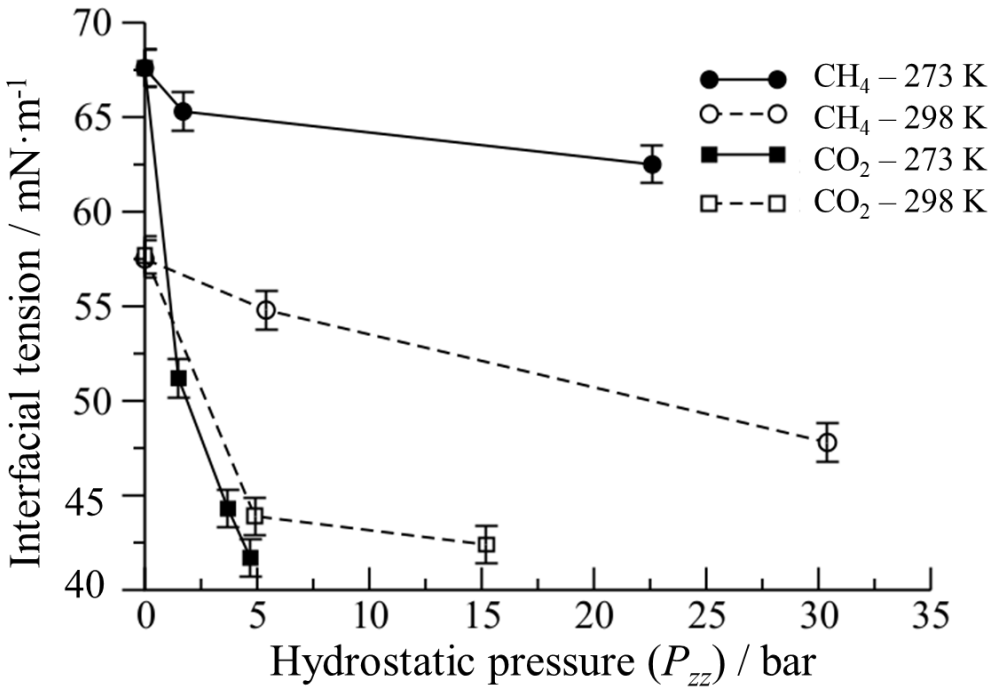

FIG. 6. The calculated interfacial tension of TBAB(aq)/pure gas systems at different hydrostatic pressures (P_{zz}) at 273.15 K and 298.15 K.

Figures 4(b), and 4(d) show that at similar gas pressures, greater numbers of CH_4 and CO_2 molecules aggregate at the TBAB solution interface compared to pure water. The presence

of TBAB in the solution leads to an increase of 20-100% in the adsorption percent of gas molecules at the interface compared to gas/water systems at similar pressures.[22,23] From Table II, the adsorption of CH_4 molecules on the TBAB(aq) solution increases as much as 22-100% compared to that of pure water, while it the adsorption percent increases up to 22% for the CO_2 systems in the TBAB(aq) compared to pure water. From comparison of two different gas-TBAB(aq) systems at the same pressures, 65% more CO_2 than CH_4 molecules are adsorbed at the interface, while 78% more CO_2 than CH_4 molecules are adsorbed at the pure water interface.

The TBAB(aq) interface exposed to CO_2+CH_4 gas mixtures was also simulated. The *z*-density profiles for water, CH_4, CO_2, Br^-, and TBA^+ in the (CO_2+CH_4)/TBAB(aq) system at the total hydrostatic pressure of 18.4 bar and 298.15 K is shown in Fig. 7. The composition of the gas mixture was chosen to give an average equilibrated $x_{CO2} \approx 0.35$ mole fraction of CO_2 in the gas phase. The concentrations of CO_2 and CH_4 are greatly enriched at the solution interface and CO_2 is adsorbed preferentially compared to CH_4, giving it a higher absolute surface density.

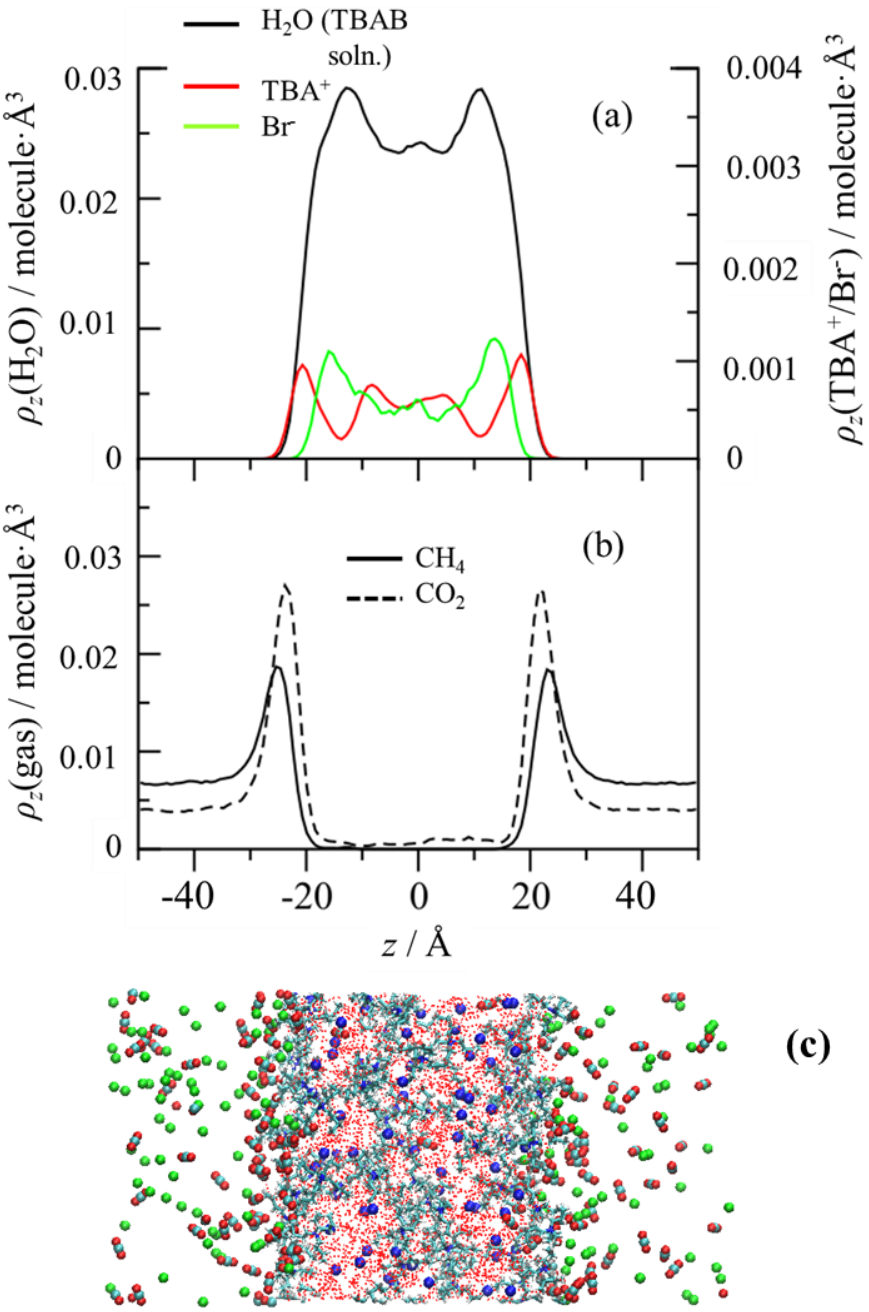

FIG. 7. The *z*-density profiles for (a) water, Br^{-}, TBA^{+} (atom C), (b) CH_4, and CO_2, in the water-TBAB/(CO_2+CH_4) system ($x_{CO2} \approx 0.35$) at the total hydrostatic pressure of 18.4 bar and 298.15 K. (c) A snapshot for the equilibrated system.

The calculated interfacial tension and molecules adsorbed on the interface from the gas mixture are given in Table III. With a given proportion of CO_2 and CH_4 molecules in the gas phase, the concentration of CO_2 molecules on the surface is enriched ~1.7 times compared to that of CH_4, specifically, the mole fraction of CO_2 at the interface is ~0.63 compared to 0.35 in the gas phase. The proportion of the adsorbed molecules at the TBAB(aq) interface varies between about 57-74% and 32-43% for the CO_2 and CH_4 components, respectively, while at the pure water interface, these values were 21-64% and 0.8-26% for CO_2 and CH_4, respectively.[23]

TABLE III. The calculated interfacial tension, γ, ($mN \cdot m^{-1}$) (with uncertainties of 1 $mN \cdot m^{-1}$) at different hydrostatic pressures, P_{zz} (bar), of CH_4 and CO_2 (with uncertainties of 0.1 bar), and the simulated average number of adsorbed gas molecules, $\langle N_X(\text{ad})\rangle$, in water-TBAB/($CO_2$+$CH_4$) system with $x_{CO2} \approx 0.35$. The total number of carbon dioxide (C) and methane (M) molecules in the simulation are also given.

T / K	P_{zz}	CH_4 : CO_2	CH_4 : CO_2	CH_4		CO_2		γ
		in gas phase	at surface	$N_M(\text{tot})$	$\langle N_M(\text{ad})\rangle$	$N_C(\text{tot})$	$\langle N_C(\text{ad})\rangle$	
		mol %	mol %					
273.15	24.9[a]	71 : 29	33 : 67	133	49	133	98	61
	10.8	67 : 33	37 : 63	133	57	133	95	52
	37.4	67 : 33	36 : 64	266	103	266	184	45
298.15	18.4	62 : 38	37 : 63	133	49	133	82	48
	56.2	61 : 39	36 : 64	266	86	266	152	37

[a] for Pure H_2O/gas system

To understand the gas mixture effect on the adsorption behavior of the each gas molecule on the TBAB(aq) interface, the results were compared with those obtained with pure gases at the same approximate pressures in Table IV. In the mixtures, the partial pressure of the gas molecules was the reference pressure used for comparing adsorption. Similar to the case of the water/gas mixture interface, there is a negative deviation between the simulated interfacial tension of the mixture and the interfacial tension calculated for an ideal mixture of gases with the specified partial pressures. This effect may be due to interactions between surface molecules in the mixture and competition between different gas species to occupy the interface.[22,23]

TABLE IV. The adsorption percent of the gas molecules in TBAB(aq)/pure gas and TBAB(aq)/ gas mixture systems at different total hydrostatic pressures, P_{zz} (bar), of CH_4 and CO_2 mixtures (with uncertainties of 0.1 bar).

Gas	**T / K**	**Mixed gas-TBAB(aq) solution**		**Pure gas-TBAB(aq) solution**	
		P_{zz} [a]	Adsorption %	P_{zz}	Adsorption %
CH_4	273	24.9	39	22.6	43
	298	34.3	32	30.4	38
CO_2	273	3.6	71	3.7	75
	298	6.9	62	4.9	66

[a] Partial pressures in the gas phase

Snapshots of the motion of single Br^- and TBA^+ ions in the solution, and CH_4 and CO_2 molecules at 298.15 K for the gas mixture system are shown in Fig. 8. Consistent with the *z*-density plots of Fig. 7, the TBA^+ and Br^- ions are not homogeneously distributed in the solution with respect to the *z*-direction, with the TBA^+ ions at greatest density at the interface and the Br^- ions spaced near the peak of the water molecules. The TBA^+ ions have strong interaction with gas molecules at the surfaces.

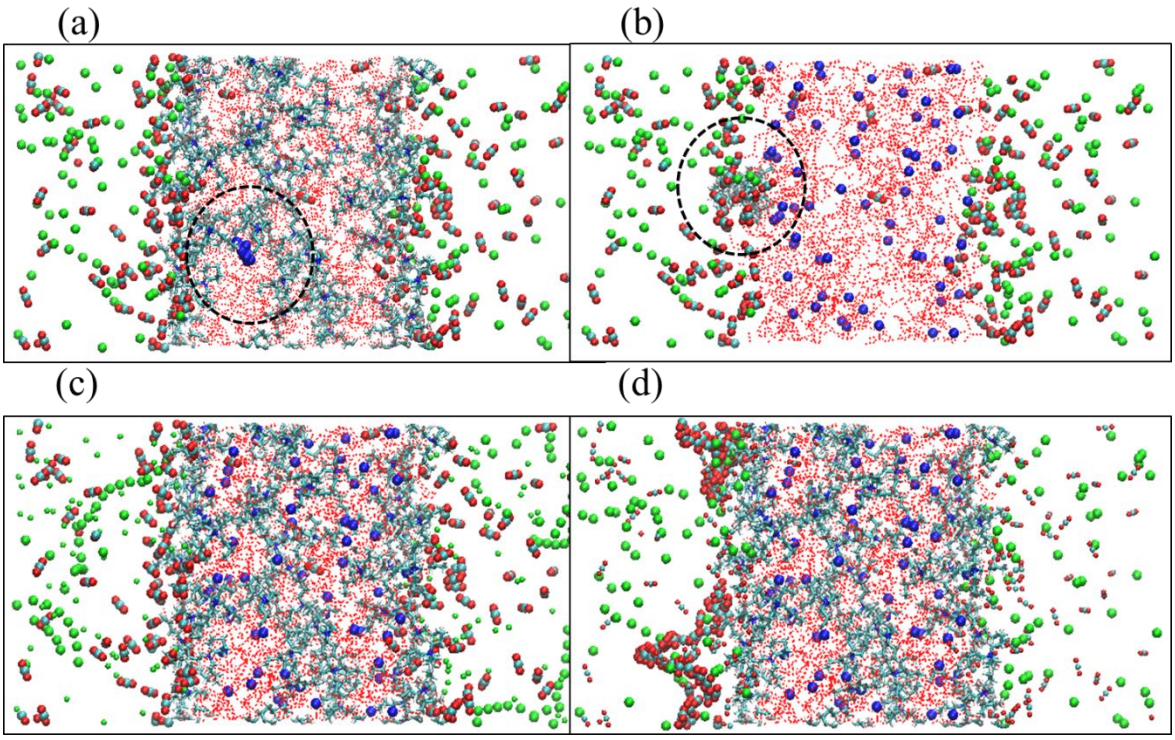

FIG. 8. Traces of snapshots of the motion of a single (a) Br^- and (b) TBA^+ ion, and (c) CH_4 and (d) CO_2 molecules over 0.5 ns at 298.15 K in the water/TBAB-gas mixture system. Other than the molecule chosen for drawing the trace, the other molecules in the system are shown at the initial configuration.

Figure 9 gives a characterization of the TBAB(aq)/gas mixture interface structure as shown by oxygen (water)-gas carbon (CH_4 or CO_2), Br^-gas carbon (CH_4 or CO_2) and nitrogen or carbon (TBA^+)-carbon (CH_4 or CO_2) radial distribution functions (RDFs) of the system. Distinct peaks are observed for N and C (TBA^+)-gas carbon RDFs, while the RDFs of oxygen (water)-gas carbon appear as small diffuse peaks. The RDFs confirm that gas molecules interact more strongly with TBA^+ ions compared to water molecules at the interface and the cations provide additional favorable interactions for the gas molecules to adsorbed at the interface. As the Br^- ions are not positioned at the interfaces, according to the *z*-density plots of Fig. 7, there are no significant peaks in the (Br^-)-gas carbon RDFs.

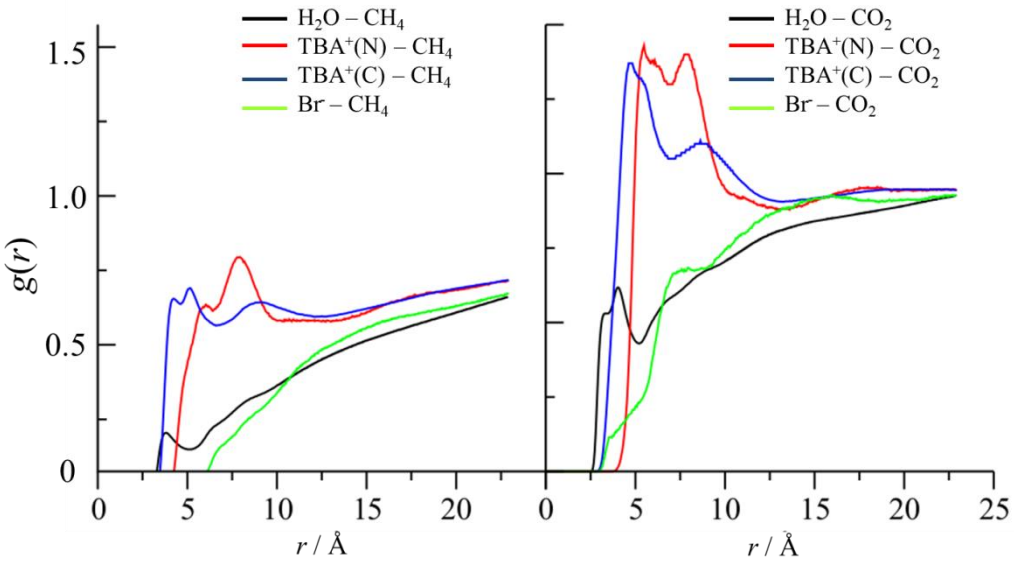

FIG. 9. Radial distribution function, $g(r)$, of the gas mixture/TBAB(aq) system for (a) CH_4 and (b) CO_2 at 273.15 K and P_{zz}=10.8 bar.

Figure 10 shows the configuration of the equilibrated TBAB aqueous solutions viewed in the *xy*-plane which is perpendicular to the surface. A portion of the TBAB(aq) interface is covered by TBA^+ and the alkyl groups of the TBA^+ ions concentrated at the interface tend to

align in the plane of the surface, so that each cation assumes the shape of an oblate spheroid whose principal axis is normal to the surface.[15] Despite the large presence of water molecules at the surface, the gas adsorption was affected by both water molecules and TBA^+ ions at the solution surface. Massoudi and King stated that hydrophobic interactions exists between alkylammonium cations concentrated at the surface and adsorbed gas molecules, and this interaction has a salting-on effect for hydrocarbon gases and salting-off effect for hydrophilic gases.[12] TBAB can therefore highly improve the CH_4 adsorption at the surface compared to that in pure water.

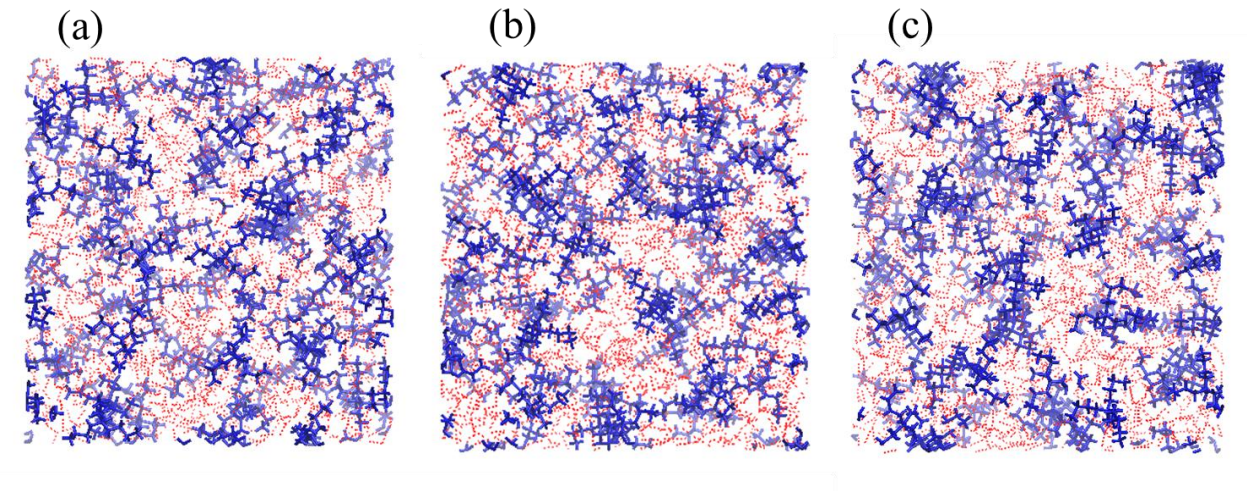

FIG. 10. The configuration of the equilibrated (a) TBAB(aq) solution not exposed to gas and TBAB aqueous solution with exposed surface at gas mixtures of (b) 18.4 bar and (c) 56.2 bar at 298 K viewed in the *xy*-plane. Water molecules are indicated by red hydrogen bonds. TBA^+ ions are shown with blue line structures with surface cations show bolder.

IV. CONCLUSIONS

The simulations in this work show that the presence of TBAB in the aqueous phase decreases the solution interfacial tension compared to pure water. This is opposite the trends for

simple salts such as NaCl which increase the interfacial tension of the aqueous solution. TBAB solutions also increase the adsorption of CH_4 and CO_2 gases at the interface. These factors may contribute facilitating the uptake of the CH_4 and CO_2 gases into the small D cages during the process of semiclathrate hydrate formation under lower pressure conditions compared to those of the pure hydrate formation.[6] As shown in Fig. 11(a) from Joshi et al., the phase diagram of the TBAB+CH_4 semiclathrate hydrate is shifted to higher temperatures and lower pressures compared to the pure structure I CH_4 clathrate hydrate.[40] The semiclathrate hydrate formation conditions become milder as the concentration of TBAB in the aqueous phase increases. The phase diagram of the TBAB+gas systems are shown in Fig. 11(b) from Muromachi et al. where it is observed that the TBAB+CH_4+CO_2 semiclathrate hydrates showed higher equilibrium temperatures (around 1 K) and lower pressures than the separate TBAB+CH_4 or TBAB+CO_2 semiclathrate hydrates.[6] Despite the higher concentration of CO_2 at the TBAB(aq) interface, the phase diagrams of Fig. 11(b) show that the TBAB + CH_4 semiclathrate hydrates form under milder conditions than the TBAB + CO_2 semiclathrate hydrates. This is likely due to the larger size of the CO_2 guests and the greater difficulty of accommodating them in the small D cages of the TBAB semiclathrate hydrate structure. Single crystal X-ray diffraction structure determination also verifies that in all D cages of the TBAB phase, there is a greater net uptake of CH_4 than CO_2.[6]

From a comparison with Fig. 11(a), the gas pressures simulated in this work (with TBAB mole and mass fractions of 0.03 and 0.32, respectively) are less than those of semiclathrate hydrate formation at the 298 K, but may be within the semiclathrate hydrate stability zone at 273 K.

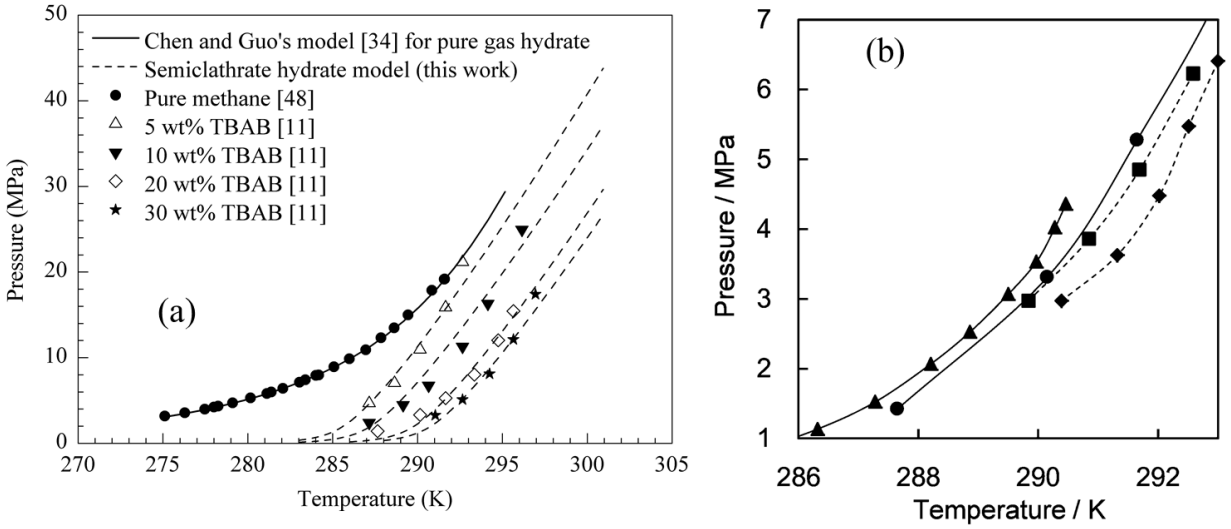

FIG. 11. (a) Phase diagrams of CH_4 structure I hydrate and TBAB + CH_4 hydrate formed from solutions with different concentrations of TBAB.[27] Reproduced with permission from Elsevier. (a) Phase diagram for TBAB + CH_4 and/or CO_2 hydrates from solutions with different mole fractions of TBAB, x_{TBAB}. In the case of gas mixtures, the mole fraction of CO2 in the gas phase, y_{CO2}, is also given. ▲, TBAB + CO_2 hydrate with x_{TBAB} = 0.013; ●, TBAB + CH_4 hydrate with x_{TBAB} = 0.014; ♦, TBAB + CH_4 + CO_2 hydrate with x_{TBAB} = 0.014, y_{CO2} = ~0.55; ■, x_{TBAB} = 0.014, y_{CO2} = ~0.35.[6] Reproduced with permission from RSC.

In the TBAB(aq) solutions, TBA^+ and Br^- ions are inhomogeneously distributed with respect to the direction perpendicular to the interface, with the TBA^+ ions concentrated at greatest density at the interface and the Br^- ions strongly hydrated inside the bulk of the solution. The surface tension of TBAB(aq) solutions with molar composition similar to the semiclathrate hydrate phases, is 7-30% less that in the surface tension of a pure water phase depending on the temperature.

The surface density of CH_4 and CO_2 gas molecules at TBAB(aq) solutions is 20-100% greater than at the surface of pure water. The adsorption of CH_4 gas on the TBAB(aq) interface is enhanced to a greater proportion compared to the pure water systems, but the absolute adsorption of CO_2 remains greater in both systems.

At the mole ratio of the solutions, it was observed that almost less than half of the TBAB(aq) interface is covered by TBA^+ and the remaining interface is water. Gas adsorption is affected by both species. Since the hydrophobic interactions exists between alkylammonium cations concentrated at the surface and adsorbed gas molecules, the TBAB solutions improve the CH_4 adsorption at the surface compared to pure water.

A combination of all of the effects described in this work can impact the mechanism of TBAB semiclathrate hydrate formation in the absence and presence of small gas molecules and help in custom tuning conditions of gas capture and other applications of these materials in areas like cold energy storage.

SUPPLEMENTARY MATERIAL

See the supplementary material for figures of the initial confirmation of the simulation cell and the equilibrated configurations at 500 K (Fig. S1), the time dependence of the total potential energy and pressure for a sample water-TBAB-CH_4 system (Fig. S2), the *z*-density profiles for TBA^+ (atom N) (Fig. S3) and *z*-density profiles for the system at higher pressures (Fig. S4), and a zoomed view of the TBAB(aq) solution in contact with CH_4 and CO_2 gas phases (Fig. S5).

ACKNOWLEDGMENTS

The authors acknowledge computational resources from the Digital Research Alliance of Canada.

AUTHOR DECLARATIONS

Conflict of Interest

The authors have no conflicts to disclose.

DATA AVAILABILITY

The data that support the findings of this study are available from the corresponding author upon reasonable request.

REFERENCES

[1] H. Hashimoto, T. Yamaguchi, H. Ozeki, and S. Muromachi, "Structure-driven CO_2 selectivity and gas capacity of ionic clathrate hydrates," Sci. Rep. **7**, 17216 (2017).

[2] S. Fan, Q. Li, J. Nie, X. Lang, Y. Wen, and Y. Wang, "Semiclathrate Hydrate Phase Equilibrium for CO_2/CH_4 Gas Mixtures in the Presence of Tetrabutylammonium Halide (Bromide, Chloride, or Fluoride)," J. Chem. Eng. Data **58**, 3137-3141 (2013).

[3] J. A. Ripmeester, S. Takeya, and S. Alavi, "Structures of Noncanonical Clathrates and Related Hydrates. In Clathrate Hydrates: Molecular Science and Characterization," J. A. Ripmeester, and S. Alavi (Eds.), Wiley-VCH, Weinheim, Germany (2022).

[4] A. Torres Trueba, "Phase behavior, kinetics and structural aspects of (semi-) clathrate hydrate systems," PhD thesis, Technische Universiteit Eindhoven (2014).

[5] M. Arjmandi, A. Chapoy, and B. Tohidi. "Equilibrium data of hydrogen, methane, nitrogen, carbon dioxide, and natural gas in semi-clathrate hydrates of tetrabutylammonium bromide," J. Chem. Eng. Data **52**, 2153-2158 (2007).

[6] S. Muromachi, K. A. Udachin, S. Alavi, R. Ohmura, and J. A. Ripmeester, "Selective occupancy of methane by cage symmetry in TBAB ionic clathrate hydrate," Chem. Commun. **52**, 5621 (2016).

[7] L. Shi, X. Shen, J. Ding, and D. Liang, "Experimental Study on the Formation Kinetics of Methane Hydrates in the Presence of Tetrabutylammonium Bromide," Energy Fuels **31**, 8540-8547 (2017).

[8] O. Nashed, J. C. H. Koh, and B. Lal, "Physical-chemical properties of aqueous TBAOH solution for gas hydrates promotion. Procedia Engineering **148**, 1351 – 1356 (2016).

[9] Z. M. Aman and C. A. Koh, “Interfacial Phenomena in Gas Hydrate Systems”, Chem. Soc. Rev. **45**, 1678-1690 (2016).

[10] I. U. Haq, A. Qasim, B. Lal, D. B. Zaini, K. S. Foo, M. Mubashir, K. S. Khoo, D-V. N. Vo, E. Leroy, P. L. Show, “Ionic liquids for the inhibition of gas hydrates. A review”, Environ. Chem. Lett. **20**, 2165–2188 (2022).

[11] L. Zhang, S. Zhou, S. Wang, L. Wang, and J. Li, “Surfactant Surface Tension Effects on Promoting Hydrate Formation: An Experimental Study Using Fluorocarbon Surfactant (Intechem-01) + SDS Composite Surfactant”, J. Environ. Protect. **4**, 42-48 (2013).

[12] H. Akiba and R. Ohmura, “Surface tension between CO_2 gas and tetra-n-butylammonium bromide aqueous solution,” J. Chem. Thermodynamics **92**, 72–75 (2016).

[13] H. Akiba and R. Ohmura, “Interfacial tension between (CO_2 + N_2) gas and tetrabutylammonium bromide aqueous solution,” J. Chem. Thermodynamics **97**, 83–87 (2016).

[14] K. Tamaki, “The Surface activity of tetrabutylammonium halides in the aqueous solutions,” Bull. Chem. Soc. Jpn. **40**, 38-41 (1967).

[15] R. Massoudi and A. D. King Jr., “Effect of pressure on the surface tension of aqueous solutions. Adsorption of hydrocarbon gases, carbon dioxide, and nitrous oxide on aqueous solutions of sodium chloride and tetrabutylammonium bromide at 25.deg,” J. Phys. Chem. **79**, 1670-1675 (1975).

[16] H. Sarlak, A. Azimi, S. M. Tabatabaee Ghomshe, M. Mirzaei, “Effect of TBAB and SDS surfactants on the interfacial tension of CO_2 Hydrate in water”, Eurasian Chem. Commun. 319-328 (2020).

[17] P. Venkataraman, “Investigation of molecular hydrophobicity for energy and environmental applications: simulations and experiments,” PhD dissertation, Tulane University (2014).

[18] S. Muromachi, K. A. Udachin, K. Shin, S. Alavi, I. L. Moudrakovski, R. Ohmura, and J. A. Ripmeester, "Guest-induced symmetry lowering of an ionic clathrate material for carbon capture," Chem. Commun. **50**, 11476 (2014).

[19] N. N. Nguyen , A. V. Nguyen, K. T. Nguyen, L. Rintoul, and L. X. Dang, "Unexpected inhibition of CO_2 gas hydrate formation in dilute TBAB solutions and the critical role of interfacial water structure", Fuel **185**, 517–523 (2016).

[20] W. Smith and T. R. Forester, "DL_POLY_2.0: A general purpose parallel molecular dynamics simulation package," J. Mol. Graphics **14**, 136-141 (1996).

[21] J. L. F. Abascal, and C. Vega, "A general purpose model for the condensed phases of water: TIP4P/2005," J. Chem. Phys. **123**, 234505 (2005).

[22] M. G. Martin and J. I. Siepmann, "Transferable potentials for phase equilibria. 1. United-atom description of n-alkanes," J. Phys. Chem. B **102**, 2569-2577 (1998).

[23] J. J. Potoff and J. I. Siepmann, "Vapor-liquid equilibria of mixtures containing alkanes, carbon dioxide and nitrogen," AIChE J. **47**, 1676-1682 (2001).

[24] J. Wang, R. M. Wolf, J. W. Caldwell, P. A. Kollman, and D. A. Case, "Development and testing of a general AMBER force field," J. Comput. Chem., **25**, 1157-1174 (2004).

[25] C. M. Breneman and K. B. Wiberg, "Determining atom-centered monopoles from molecular electrostatic potentials. The need for high sampling density in formamide conformational analysis," J. Comput. Chem.. **11** (3): 361 (1990).

[26] H. Docherty, A. Galindo, C. Vega, and E. Sanz, "A potential model for methane in water describing correctly the solubility of the gas and the properties of the methane hydrate," J. Chem. Phys. **125**, 074510 (2006).

[27] P. Naeiji, T. K. Woo, S. Alavi, F. Varaminian, and R. Ohmura, "Interfacial Properties of Hydrocarbon/Water Systems Predicted by Molecular Dynamic Simulations," J. Chem. Phys. **150**,114703 (2019).

[28] P. Naeiji, T. K. Woo, S. Alavi, and R. Ohmura, "Molecular dynamics simulations of interfacial properties of the CO_2–water and CO_2–CH_4–water systems," J. Chem. Phys. **153**, 044701 (2020).

[29] M. M. Conde and C. Vega. "Determining the three-phase coexistence line in methane hydrates using computer simulations." J. Chem. Phys. 133, 064507 (2010).

[30] J. M. Míguez, M. M. Conde, J.-P. Torré, F. J. Blas, M. M. Piñeiro, and C. Vega. "Molecular dynamics simulation of CO_2 hydrates: Prediction of three phase coexistence line". J. Chem. Phys. 142, 124505 (2015).

[31] J.P.R.B. Walton, D.J. Tildesley, J.S. Rowlinson, and J.R. Henderson. "The pressure tensor at the planar surface of a liquid". Mol. Phys. **48**, 1357-1368 (1983).

[32] J. Alejandre, D. J. Tildesley, and G. A. Chapela, "Molecular dynamics simulation of the orthobaric densities and surface tension of water," J. Chem. Phys. **102**, 4574 (1995).

[33] F. Biscay, A. Ghoufi, V. Lachet, and P. Malfreyt, "Monte Carlo calculation of the methane-water interfacial tension at high pressures," J. Chem. Phys. **131**, 124707 (2009).

[34] F. Biscay, A. Ghoufi, V. Lachet, and P. Malfreyt, "Monte Carlo calculation of the pressure dependence of the water-acid gas interfacial tensions." J. Phys. Chem. B **113**, 14277-14290 (2009).

[35] A. Ghoufi and P. Malfreyt. "Calculation of the surface tension of water: 40 years of molecular dynamics". Mol. Simul. **45**, 295-303 (2018).

[36] A. Ghoufi, P. Malfreyt, and D. J. Tildesley. "Computer modelling of the surface tension of the gas-liquid and liquid-liquid interface". Chem. Soc. Rev. **45**, 1387-1409 (2016).

[37] S. Alavi, “Molecular Simulations: Foundations and Practice,” Wiley-VCH, Weinheim, Germany (2020).

[38] M. Perumal, A. Balraj, D. Jayaraman, and J. Krishnan, “Experimental investigation of density, viscosity, and surface tension of aqueous tetrabutylammonium-based ionic liquids,” Environ. Sci. Pollut. Res. **28**, 63599–63613 (2020).

[39] X. Wang, C. Chen, K. Binder, U. Kuhn, U. Pöschl, H. Su, and Y. Cheng, “Molecular dynamics simulation of the surface tension of aqueous sodium chloride: from dilute to highly supersaturated solutions and molten salt.,” Atmos. Chem. Phys. **18**, 17077-17086 (2018).

[40] A. Joshi, P. Mekala, and J. S. Sangwai, “Modeling phase equilibria of semiclathrate hydrates of CH_4, CO_2 and N_2 in aqueous solution of tetra-n-butyl ammonium bromide,” J. Nat. Gas Chem. **21**, 459–465 (2012).